DETERMINATION OF IRON CORE LOSSES UNDER INFLUENCE OF THIRD HARMONIC FLUX COMPONENT

* P. Rupanagunta, J.S. Hsu, and W.F. Weldon

Abstract: The core loss for a magnetic material under excitation can be estimated from the flux density vs. the field-strength loops or B-H loops. A method is presented for predicting the position, size, and the number of minor loops formed in the B-H loop, while harmonics of known magnitude and phase angle occur along with the fundamental, under distorted excitation. The data required for this method is a set of B-H loops at the fundamental excitation frequency and loops formed under third harmonic excitation frequencies, over a range of flux densities.

INTRODUCTION

Magnetic fluxes encountered in rotating electric machines are frequently found to contain odd harmonics, of which the third harmonic is dominant.[1] For example, the third-harmonic flux exists due to saturation in rotating machines. A three-phase transformer with independent magnetic paths, contains third-harmonic flux and shows minor loops in its hysteresis curve in spite of being fed purely sinusoidal voltage.[2] The relative magnitudes and phase angles of the harmonic components in the flux-density waveform affect the core losses.

Core losses in magnetic materials used in electrical equipment are caused by the eddy current and hysteresis phenomena.[3, 4, 5, 6, 7] The former depends on certain factors such as effective voltage across the exciting terminals, the frequency of the flux variation, and the resistance of the magnetic circuit. Nakata [8] has suggested that the hysteresis loss for a given excitation frequency in a given material is fixed for a particular peak-flux density which, in turn, depends

---

* This work was supported by the National Science Foundation through Grant No. ECS-880884 and partially by the State of Texas through Grant No. 1591.

The authors are with the Center for Electromechanics, The University of Texas at Austin, Austin, TX 78758.

on the harmonic content of the flux. This has been found in agreement with the tests conducted by the authors, for situations where there are no minor loops in the B-H loop. The total iron losses can be determined for any given frequency by measuring the area of the B-H loop, i.e. the flux density vs. the field-strength loop.

Core-loss data are typically provided by manufacturers in graphical form with induction (in Tesla) plotted against core loss (in W/kg) for different materials. Also available are the B-H loops for particular excitation frequencies with induction on one axis and magnetizing force on the other.[9] When the relative phase angles of the harmonic fluxes, with respect to the fundamental flux density waveform are not taken into consideration, simple mathematical addition of core losses due to each harmonic component from the manufacturer's data charts may result in inaccurate values of loss in the material under excitation. This is because the losses mentioned are dependent on the resultant flux waveform.

From figure 1a, if the fundamental and the third harmonic are in phase, the resultant has peak value at A; while, if the third harmonic is 90° lagging, the peak value (fig. 1b) is at B. The losses are different due to the effect of the change in peak flux on the hysteresis loss.

When measuring the core losses by means of transformer setups, even when the applied voltage is sinusoidal, it is possible that the back electromotive force (EMF) may deviate from the sinusoidal waveform. This is due to the leakage impedance in the winding. The amount of distortion increases as the saturation value is approached.

Research efforts over the past few years in analyzing iron-loss behavior have resulted in steadily improving loss models accurate over wider ranges of excitation conditions and materials. Iron losses under distorted waveform conditions have been measured, but not explained by Wada.[10] Asner [11] has explained the effect of harmonic waves in terms of waveform factor. While Hemmer [12] discusses the relation between waveform and distortion factors in experimental and analytical terms, his measurements are confined to a particular phase angle.

Nakata [8] analyzed the relationship between the waveform factor of the voltage, the distortion factor of the flux wave, and the effect of amplitude and phase angle of the harmonics relative to the fundamental on the minor-loop characteristics. A formula was developed which expresses the relation between the distortion factor and the iron losses. His experiments show that hysteresis losses are proportional to the maximum-flux density, while the eddy-current losses are proportional to effective voltage. The flux density is given as:

$$B = K\int v(\omega t)d(\omega t) \tag{1}$$

where

K = proportionality constant
$v(\omega t)$ = back EMF across the winding
ω = angular frequency of exciting EMF
B = flux density in material

In general, the distorted voltage, v(wt) can be expressed as the Fourier series:

$$v(\omega t) = v_1\left(\sin[\omega t + \theta_1]\right) + v_3\left(\sin[3\omega t + \theta_3]\right) + \ldots$$

$$+v(2n+1)\left(\sin\left[(2_{n+1})\omega t + \theta_{2n+1}\right]\right) + \ldots \tag{2}$$

where

$n = 1, 3, 5$
$V_n = n^{th}$ harmonic back EMF across the winding
θ_n = phase angle in radians for the n^{th} harmonic component

The flux density waveform can be expressed as:

$$B(\omega t) = K\{-v_1\left(\cos[\omega t + \theta_3]\right) - v_3\left(\cos[3\omega t + \theta_3]\right)/3$$

$$-v(2_{n+1})\left\{\cos\left[(2n+1)\omega t + \theta_{3n+1}\right]\right\}/(2n+1) + \ldots\} \tag{3}$$

The above equation is used to calculate the flux density in the material under harmonic excitation.

The objective of this paper is to present a generalized model to predict the core losses in the magnetic material under any specified conditions of magnitudes and phase angles of the harmonics in the flux-density waveform. The model is based on a combination of theoretical and empirical approaches. Results based on extensive experiments, particularly, using third-harmonic flux are presented. The experimental efforts have focused mainly on a single harmonic-flux component being present in the core. Observed and predicted results are in agreement. It is hoped that the method outlined can be extended to predict loss behavior under two or more harmonic-flux components being simultaneously present and separate investigations are to be conducted in the future.

In this paper, digital acquisition of the traces of flux density, ampere turns (AT), and the back EMF of the coil has been made in the experiments, enhancing the accuracy of measurements due to the point-by-point analysis of the trace.

EXPERIMENTAL SETUP AND DATA ACQUISITION PROCEDURE

For predicting the loss in the magnetic material, the following data has to be available:

1. B-H loops at a range of flux densities for the fundamental frequency excitation. The range of 1.0 to 1.8 T is typical of the range in which machines are operated.
2. B-H loops at a range of flux densities under excitation at harmonic frequencies of interest.
3. The dc-hysteresis loop at a range of flux densities. This loop represents the hysteresis loss in exclusion of eddy-current loss.

Three C-core transformers [8], with two windings each, are used (fig. 2) to have reasonably uniform flux density. Each transformer is tape wound with cold-rolled grade, 4-mil thick, 3%-Si [13] laminations. These AH-25 cores, from Arnold Electric Co., have a nominal weight of 1.398 kg each. The C-core is made by winding a Silicon steel strip on a mandrel to make a gapless core. The core is

annealed to relieve winding stresses and impregnated with varnish for rigidity. This core is cut into two halves and carefully processed so that the two halves are accurately dimensioned and the effective air-gap at the butt-joint is very small. The butt joint of the clamped C-cores is lapped such that the maximum effective airgap is 0.5 mil. The transformer cores are clamped together according to the manufacturers' suggestion at 272 kg.

The strips in the core are electrically insulated from each other by a film of Magnesium Oxide (C-10 finish). This provides exceptionally good interlaminar resistance with negligible space factor. The strips are not magnetically insulated from each other.

The primary windings are connected in star and 3 phase, 60-Hz voltage, is fed to these windings. The secondary windings are connected in series delta. The third-harmonic source is applied to the secondary windings as shown in figure 3.

Apart from being wound with two main coils, the primary and secondary of 60 turns each, the core subject to test is wound with a search coil of five turns. The search coil signal goes through a passive integrator which is a series resistance-capacitance (RC) circuit. The flux signal is obtained by connecting a probe across the terminals of the capacitive element. Since the alternating current voltage passing through the capacitance is integrated according to equation (1), the flux density is obtained as described,

$$R = 300\ k\Omega$$
$$C = 0.6\ \mu F$$
$$20\ \mu F \text{ for low (2 Hz) frequency test}$$

While one of the main coils is for fundamental-frequency excitation, the other is for third-harmonic excitation. The third harmonic frequency signal is a zero sequence or single-phase quantity and the current can thus flow in delta. If we supply balanced, three-phase fundamental frequency voltages to the star connected windings, then the induced fundamental frequency EMFs are summed to zero in the delta. The third-harmonic flux in the magnetic path can be independently controlled by varying the magnitude and the phase angle of the third-harmonic voltage applied to the delta circuit.

If the neutral of the fundamental frequency, star-connected coils is left isolated from the power supply neutral, the star-connected coils are an open circuit as far as the third-harmonic current is concerned. Then, the third-harmonic current (being zero-sequence) cannot flow in the fundamental frequency coils. Therefore, the fundamental and third-harmonic circuits operate without interference from each other.

The third-harmonic voltage is fed into the secondary windings. A microprocessor generated pulse train of third-harmonic frequency is filtered and amplified; the amplifier output is fed to the secondary windings. The magnitude and the phase angle that the third-harmonic voltage bears to the fundamental can be manually adjusted over a wide range. The test circuit setup is shown in figure 4.

Calibration of the Digital Oscilloscope

For the experiments, two signals were measured and calibration was carried out as follows:

Flux Density

The terminals of the search coil across the test core were connected across an RC integrator; the capacitor leads were hooked up to the Y channel of the scope. Known fundamental single phase, ac voltage required to allow 1 T, at which the core material is unsaturated, measured from the search coil was fed to the core. The harmonic content of the voltages across the search coil was checked on the spectrum analyzer and harmonic percentage was negligible compared to the fundamental. The trace on the scope was thus calibrated for flux density. The fundamental voltage of the search coil can be determined from the equation:

$$e = 4.44\,(f\ N\ A\ B)V \tag{4}$$

where

e = back EMF of search coil
f = frequency of excitation
N = number of search coil turns
A = area of cross section of the core
B = flux density in Tesla in the core

Ampere-Turns

A known dc current was applied across a known ohmic resistance of 0.01 Ω. The resistance used has an accuracy of better than 0.025% of range per degree Celsius between 0 to 50° and a frequency response from dc to 20 kHz.

The voltage across the resistance was measured and the scope terminals were connected across the terminals of the resistance. Switching on the dc current resulted in a deflection on the scope, thereby yielding an accurate method to estimate the amperes and, hence, the AT in the circuit.

The waveforms of the flux density B (in Tesla) and the AT are obtained and stored in the memory of a digital scope. This storage of each waveform is in the form 1,024 data points. Each data point is assigned an integer value within the limits of 128 and -127, as the scope has a vertical resolution of eight bits. These data points are transferred to the computer, in this case an IBM-PC, using the GPIB [14] corresponding to the IEEE 488 specification. Array transfer, manipulation, and array format conversion is carried out using the Asystant software [15]. Use is made of the same software to plot B-H loops, while FORTRAN code is used to compute the areas covered by the loops. It may be mentioned that the data-acquisition method is applicable over a wide range of core materials, as well as in situations where C cores are not used.

EXPERIMENTAL METHOD

To obtain the categories of data as listed in the section above, the following experimental procedure was adopted.

Under single-frequency excitation, at 60 and 180 Hz, core loss was measured using digital wattmeters, as well as by calculation of the area of the B-H loops as described later. Tests in the sample study were performed at a sequence of flux densities, starting from 1 to 1.6 T (fig. 5a, 5b).

Next, under carefully controlled injection of third-harmonic voltage along with the 60-Hz voltage, the critical condition for minor-loop formation was reached. It was observed that when the B waveform had the presence of more than two points, where the rate of flux change was zero (i.e., dB/dt = 0), the B-H loop (fig. 6b) showed a pair of incursions. The dc-hysteresis loop, where there is no eddy-current loss involved, is obtained by means of very low-frequency excitation, and closely approximates the dc-hysteresis loop. A set of such loops, over a range of flux densities, were experimentally obtained.

When the magnitude of the third harmonic was raised, minor-loop formation started. The presence of minor loops indicates an additional loss in the core, corresponding to the proportion of the area under the minor loops.

The step up transformer was selected to operate at the nonsaturated region; consequently, it does not contribute any significant distortion of the harmonic frequency.

OBSERVATIONS

In the first cycle of experiments, B-H loops at 60-Hz excitation without presence of harmonics were obtained. B-H loops at 180 Hz were also obtained (table 1). The static-hysteresis loops (i.e., for dc excitation) were obtained for a range of flux densities.

The copper (i^2r) losses occurring in the conducting wires to the transformer windings, as well as in the windings themselves, are subtracted from the wattmeter readings. Next, the B-H loop for the condition of critical appearance of the minor loop was obtained. This occurs when the B waveform begins to exhibit more than two points where the slope of the curve is zero. Here, the rate of change of flux, dB/dt = 0 (a finite number of points representing the waveform of B), had the same numerical value. Corresponding to these points, there was observed a single point on the AT waveform whose slope was zero (fig. 6a). This

implies that the rate of change of flux with respect to current was zero at this particular point, that is di/dt = 0; the B-H loop shows a pair of regions where there are incursions (fig. 6b).

By using experimental evidence, we can say that the points described above lie on the dc-hysteresis loop. Previously, efforts have been made in this direction by researchers.[9] In other words, the points indicate the locus of purely hysteresis losses, this locus coincides with the static hysteresis loop (fig. 6c).

The experimental data also indicates that if the harmonic content increases such that the B waveform has a secondary crest and valley, then the minor loops will have to appear.

DETERMINING POSITION, SIZE, AND NUMBER OF MINOR LOOPS THROUGH A SAMPLE STUDY

A series of tests were conducted to use the B-H-loop data in predicting the losses under known magnitude and phase angle of third harmonic flux density. Empirical relations were derived between the data available in the form of B-H loops for single frequencies and the B-H loop observed with minor loops under nonsinusoidal excitation.

Two sets of the series of tests conducted have been presented here (table 2). The results presented on the upper row in the table are used for the following analysis and those of the second row were used for verification. The tests conducted indicate that:

1. For every occurrence of a secondary crest and valley in the flux-density waveform, a minor loop is formed in the B-H loop. In the case of the presence of third harmonic along with the fundamental, we observe two minor loops.
2. The B-H loop at 60 Hz, whose peak-to-peak value is exactly the same as the provided B waveform, is selected from the family of loops in figure 5b. This is redrawn in figure 7d.
3. The vertical bounds of the minor loops on the B-H loop can be determined from the vertical bounds of the secondary crest and valley of the B

waveform. Points P and Q refer to the secondary crest and valley on the B waveform which needs to be analyzed (fig. 7a). Since these points occur past the positive peak of the B waveform, the corresponding minor loop shall lie on the downgoing (left) part of the loop. Similarly, R and S shall be used to determine the minor loop on the lower half of the loop.

4. The lower extremity, M, of the minor loop, lying nearer the top of the B-H loop, lies exactly on the static-hysteresis curve for the corresponding flux density. Similarly, the upper extremity, N, of the minor loop lying close to the bottom of the major loop also lies on the static-hysteresis curve.
5. To reckon the horizontal spread of the loop, the following steps are taken:
   a. Select the B-H loop for the harmonic (due to which the minor loops result, in this case the third harmonic) of the same peak flux density value as the height of the secondary peak on the B waveform. A loop from figure 1b whose peak-to-peak value lies exactly between Q and S of figure 7a is selected (fig. 7b). This is based on the assumption that the rate of change of the flux density with respect to time corresponds to the third-harmonic frequency. The flux reversal must now follow the 180-Hz curve.
   b. The contour of the 180-Hz loop, Y'X'T' (fig. 7b), is used to extrapolate the curve on figure 7d from M through X. Thus, X lies on the intersection of the above contour and the parallel representing the height of the secondary peak of the B waveform; i.e. half the vertical distance from Q to R. Point X is connected to F in figure 7d by interpolation along G, using the Q'P'F' contour from figure 7b. Finally M is joined through G to the peak of the major loop in B-H loop.

This completes the positioning of the minor loop on the upper half of the B-H loop. Assuming that the B waveform is symmetrical about the time axis, the other minor loop can be constructed based on the same set of steps. N lies on the static-hysteresis loop, PNT is drawn following the Y'X'T' contour, QP follows the Q'P' contour, and Q is connected by using the contour Y'X'. Thus, the minor loops are positioned on the major loop.

By superimposing the static (dc) hysteresis loop onto the predicted B-H loop and subtracting the area of the former from the latter, the losses due to hysteresis and eddy-current phenomena are separable. This is based on the theory that hysteresis losses are constant for any two distorted waveforms whose peak-to-peak value is the same. No attempt has been made to distinguish between the hysteresis loss from the eddy-current loss in the minor loop. Losses in the minor loops consist of both above named type of losses. The hysteresis loss in the major loop is obtained and there is a hysteresis-loss component present along with the eddy-current losses. For small minor loops, this component is small compared to the total eddy-curent loss.

RESULTS

The predicted B-H loop in figure 7d is in close agreement to the one actually observed on the oscilloscope screen from the test. The dotted trace represents the predicted loop.

Moreover, the calculation of the loss from the area calculation of the B-H loop is in close agreement to the actually measured wattmeter loss reading. Results are shown on table 3.

Total loss for the B-H loop (fig. 7d) can be separated into hysteresis and eddy-current losses as described above (fig. 8c). The outer trace represents the total losses and the inner trace is the hysteresis loss. Subtracting the area of the inner trace from the outer trace, we obtain the eddy-current loss; however, a fraction of this loss is the hysteresis loss present in the minor loop. Results are presented in the section below.

B-H LOOP CALCULATION

Total instantaneous power going into coil and core:

$$v\,i = e\,i + \text{copper loss in coil} \tag{5}$$

where

v = applied instantaneous voltage
e = instantaneous back EMF
i = instantaneous current in the coil

Total energy into core per cycle:

$$\int_0^{1\,\text{cycle}} e\,i\,dt \tag{6}$$

since

$$e = N\frac{d\phi}{dt} = NA\frac{dB}{dt}$$

where

N = number of winding turns
A = area of cross section of the core
ϕ = flux in the core in Wb
B = flux density in the core in T

we can write (6) as:

Energy into core per cycle =

$$\int_0^{1\,\text{cycle}} N\frac{d\phi}{dt}\,i\,dt = \int_0^{1\,\text{cycle}} N\,A\,\frac{dB}{dt}\,i\,dt$$

rearranging,

$$A\int_0^{1\,\text{cycle}} N\,i\,\frac{dB}{dt}dt = A\int_0^{1\,\text{cycle}} (N\,i)\,dB$$

$$\text{Area of core}\int_0^{1\,\text{cycle}} (\text{ampturns})\,dB \tag{6a}$$

CONCLUSIONS

If a set of B-H loops under different flux densities for the fundamental waveform frequency and a similar set for its third harmonic is available for a core material, then the occurrence, size, and position of the minor loops can be predicted under conditions where the third harmonic of any magnitude and phase angle to the fundamental are present along with the fundamental. This points to a method of accurately predicting the core losses under nonsinusoidal excitation over a range of working flux densities. The core losses can be conveniently split into hysteresis and eddy-current losses under the assumption [8] that the hysteresis losses are proportional to maximum-flux density and the eddy current losses are proportional to effective EMF.

The method is equally applicable in core material of transformers as well as rotating electric machines. Transformers are used for the tests in order to determine the basic core losses, i.e., hysteresis and eddy-current losses for materials used in transformers as well as rotating machines. A rapid and relatively less difficult method of estimating the core losses accurately with a minimum of data and equipment is facilitated.

The prediction method is not limited by the size or the phase angle of the harmonics. Tests over the range of working flux densities of up to 1.8 T are useful in determining the losses within the same range. The process of obtaining the data described above can be computerized. This can facilitate the use of the prediction method for a large number of core materials.

The tests are limited to the presence of only one harmonic. Work is being done to extend the prediction of situations which include higher flux densities and presence of multiple harmonics.

ACKNOWLEDGMENTS

The authors would like to thank the National Science Foundation for financial support through Grant No. ECS - 880884 and the State of Texas for Grant No. 1591. The authors gratefully acknowledge their debt to Professor H. H. Woodson for his supervision and keen interest in this subject. We wish to thank

the Center for Electromechanics and the Center for Energy Studies, both at The University of Texas at Austin for their support staff and facilities provided for this research effort.

REFERENCES

[1] J.S. Hsu, H.H. Woodson, and S.P. Liou, "Experimental Study of Harmonic-Flux Effects in Ferromagnetic Materials," *IEEE Transactions on Magnetics*, vol 25, no. 3, pp 2678-2685, May, 1989.

[2] T. Nakata and Tohi, *Choguku Branch Convention of Four Institutes of Electrical Engineers*, Japan, no. 1-15.

[3] D.S. Takach and R.L. Boggavarapu, "Distribution Transformer No-load Losses," *IEEE Transactions on Power Apparatus and Systems*, pp 181-193, January, 1985.

[4] J.S. Hsu, S.S. Liou, and H.H. Woodson, "Peaked-MMF Smooth-Torque Reluctance Motors," *IEEE Transactions on Energy Conversion*, vol 5, no. 1, pp 104-109, March, 1990.

[5] J.S. Hsu, S.S. Liou, and H.H. Woodson, "Comparison of The Nature of Torque Production in Reluctance and Induction Motors," *IEEE Power Engineering Society Winter Meeting*, February, 1990.

[6] J.S. Hsu, H.H. Woodson, and S.S. Liou, "Potential for Loss Reductions in Transformers through Utilization of Third-Harmonic Flux," *IEEE Industrial Application Society Annual Meeting Conference Record:* Pittsburgh, PA, pp 1443-1450, October, 1988.

[7] S.S. Liou, "Theoretical and Experimental Study of Polyphase Induction Motors with Added Third-Harmonic Excitation," *Master's Thesis submitted to Graduate School*, The University of Texas at Austin, December, 1985.

[8] T. Nakata, et al., "Iron Losses of Si Steel Core Produced by Distorted Flux," *IEEE Transaction in Magnetics,* vol 90, no. 1, 1970.

[9] *Armco Oriented Electrical Steels: Design Manual, Armco, Inc.,* Middletown, OH, pp 1-20, 1986.

[10] Wada and Nagaoka, *Electrotechnical Papers of IEE,* Japan, vol 4, no. 12, p 483, 1943.

[11] A. Asner, "Transformer No-load Losses with Distorted Voltage Waveforms," *The Brown Boveri Review (12)*, vol 47, pp 875-882, 1965.

[12] N. Hemmer, *Electrotech. Z. (ETZ)-A,* vol 86, no. 12, p 396, 1965.

[13] S.C. Arnold, *107 B Silectron Cores*, Doc. 613-00-101 Marengo, IL, Arnold Engg, Co. (undated).

[14] *Gould 1600 Series Operators Manual,* part no. 456840, Gould, Inc. Recording Systems Division, 3631 Perkins Ave., Cleveland, OH, 1988.

[15] *ASYSTANT GPIB - The Scientific Number Cruncher*, ASYST Software Technologies, Inc., 100 Corporate Woods, Rochester, NY, 1988.

Table 1. Total losses under single-frequency excitation

Frequency From (Hz)	Inferred Flux Density Harmonic Content	Flux Density (Tesla)	Loss/kg. from Wattmeter (W)	Loss/kg. BH Loop Area (W)
60	<5%	0.8	0.20	0.18
	<5%	1.1	0.29	0.25
	<5%	1.3	0.38	0.30
	<5%	1.4	0.48	0.38
	<5%	1.6	0.62	0.47
180	<8%	0.14	0.03	0.03
	<8%	0.25	0.08	0.07
	<8%	0.42	0.20	0.20
	<8%	0.60	0.38	0.38
	<8%	0.85	0.76	0.76
	<8%	1.20	1.21	1.14

Table 2. Total losses at 1.08 T (with constant peak flux density and different phase angle between fundamental and third harmonic)

Voltage	Wattmeter (60 Hz)	Wattmeter (180 Hz)	Total Loss/kg. (W/kg)	Loss/kg from BH loop area (W/kg)
21.37	1.37	0.88	0.31	0.29
22.69	0.60	1.88	0.36	0.36

Table 3. Comparison of total losses at 1.08 T (in Watts)

Total Wattmeter Loss (W/kg)	Loss/kg from Actual BH Loop (W/kg)	Loss/lb. from Predicted BH Loop (W/kg)
0.97	0.29	0.29
1.12	0.36	0.39

Table 4. Loss separation

Total loss/kg	0.29 W
Hysteresis loss	84% or 0.24 W
Eddy current loss, with minor loop hysteresis loss component	16% or 0.05 W

VITA

William F. Weldon
Professor, Electrical and Computer Engineering
Professor, Mechanical Engineering
Director
Center for Electromechanics
Director
Center for Fusion Engineering
The University of Texas at Austin

BSES	Trinity University, San Antonio	1967
MSME	The University of Texas at Austin	1970

Professor Weldon was appointed Director of the Center for Fusion Engineering at The University of Texas at Austin in August 1988 and Director of the Center for Electromechanics at The University of Texas at Austin (CEM-UT) in 1985. Prior to that, he served as Technical Director of CEM-UT since its establishment in 1977 and as Chief Engineer of CEM-UT's predecessor, the Energy Storage Group, from 1973 to 1977. During his directorship, CEM-UT has received two honorable recognitions: designation as a United States Army Center of Excellence and designation by the United States Defense Advanced Research Projects Agency (DARPA) as an "Independent Management Activity" for the development of electromagnetic (EM) gun technology. Under his leadership, an initial investigation of inertial energy storage with homopolar conversion for magnetic fusion power supplies has expanded into a broad spectrum of electromechanical research and development projects. The Center for Electromechanics accomplishments include the development of a fast-discharging homopolar generator (HPG), three generations of conventional HPGs including the compact HPG; a HPG with superconducting excitation; three generations of compulsators (of which Professor Weldon is a co-inventor); the development of advanced machine components, especially bearings and sliding electrical contacts; an industrial applications program exploring the application of pulsed power technology to manufacturing processes including HPG pulsed resistance welding, pulsed electrical heating, electrical sintering, and EM powder spraying; and the development of EM launch technology including the first injected railgun, the distributed energy store railgun, cryogenically cooled inductive stores, high speed opening switch technology, ultrahigh velocity railguns, large scale railguns for tactical applications, and the development of advanced coaxial accelerators.

Professor Weldon has served on over 19 advisory panels and committees. His other professional experience includes seven years in industry where he was engaged in the design and development of mechanical and electromechanical prototypes. A registered professional engineer in Texas, he has been a consultant to more than 20 groups or firms since 1974, including American as well as European firms. He has authored over 235 technical publications, and holds 20 patents in the area of rotating electrical machinery and pulsed power with seven patents pending. He is listed in American Men and Women of Science, Who's Who in the South and the Southwest, Who's Who in Aviation and Aerospace, Who's Who in Frontier Science and Technology, International Who's Who in Engineering, Who's Who in Technology, and Who's Who in the World. Professor Weldon was awarded the Peter Mark Medal in 1986 for his outstanding contributions in EM launch technology.

VITA

John S. Hsu (or Htsui)
Research Engineer
Center for Electromechanics
The University of Texas at Austin

BS	Tsing-Hua University	1959
PhD	Bristol University	1969

Dr. Hsu was born in China. He received his Bachelor of Science degree from Tsing-Hua University, Peking, China and Doctor of Philosophy degree from Bristol University, Bristol, England in 1959 and 1969, respectively.

After graduation, he joined the Electrical and Electronics Engineering Department of Bradford University, England, serving there for two years. After his arrival in the United States in 1971, he worked in research and development areas for Emerson Electric Company and later for Westinghouse Electric Corporation. He served as head of the Rotating Machines and Power Electronics Program, Center for Energy Studies, The University of Texas at Austin for over four years. Presently, he is the manager of the Industrial Drives Program at the Center for Electromechanics at The University of Texas at Austin.

Dr. Hsu is a Chartered Engineer in the United Kingdom and a Registered Professional Engineer in the States of Texas, Missouri, and New York.

VITA

Paresh Rupanagunta
Graduate Research Assistant
Center for Electromechanics
The University of Texas at Austin

BSEE	Regional Engineering College	1988
MSEE	The University of Texas	

Paresh Rupanagunta was born in New Delhi, India. After completing his degree in Electrical and Electronics Engineering at the Regional Engineering College, Tiruchirapalli, India, he entered the graduate school of The University of Texas at Austin in September 1988. He is currently working toward a Master's degree and is involved with research in rotating machines at the Center for Electromechanics at The University of Texas at Austin.

FIGURE CAPTIONS

Figure 1a. Resultant flux densities plotted against time at different relative phase angles of the third-harmonic flux

Figure 1b. Resultant flux densities plotted against time at different relative phase angles of the third-harmonic flux

Figure 2. C-core transformer

Figure 3. Connection diagram

Figure 4. Schematic for test apparatus

Figure 5a. B-H loops at 60 Hz

Figure 5b. B-H loops at 180 Hz

Figure 6a. Flux-density waveform corresponding to incursions

Figure 6b. B-H loop with incursions

Figure 6c. B-H loops with comparison of incursions

Figure 6d. Locus of incursions

Figure 6e. Direct current hysteresis loop and locus of incursions

Figure 7a. Flux-density waveform to be analyzed

Figure 7b. Third-harmonic loop

Figure 7c. B-H loop from actual test

Figure 7d. Predicted B-H loop

Figure 7e. Comparing the results

Figure 8a. Predicted loop

Figure 8b. DC loop

Figure 8c. Separating the loss components

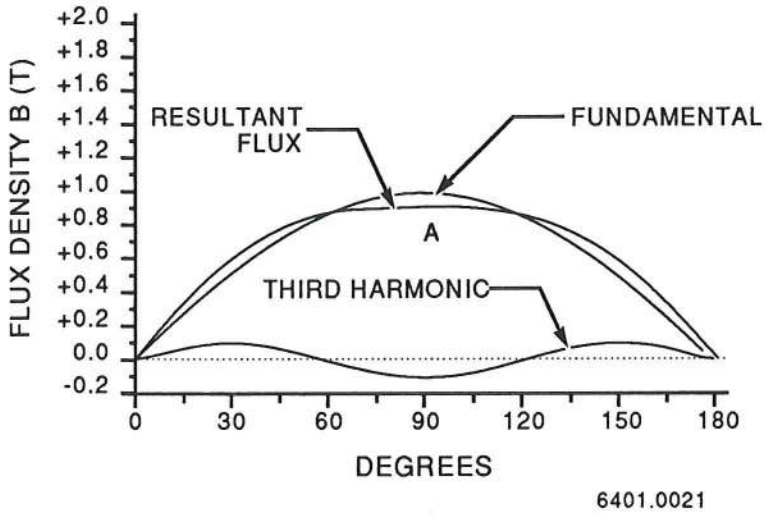
FLUX DENSITY B (T)
+2.0
+1.8
+1.6
+1.4
+1.2
+1.0
+0.8
+0.6
+0.4
+0.2
0.0
-0.2
RESULTANT FLUX
FUNDAMENTAL
A
THIRD HARMONIC
0
30
60
90
120
150
180
DEGREES
6401.0021

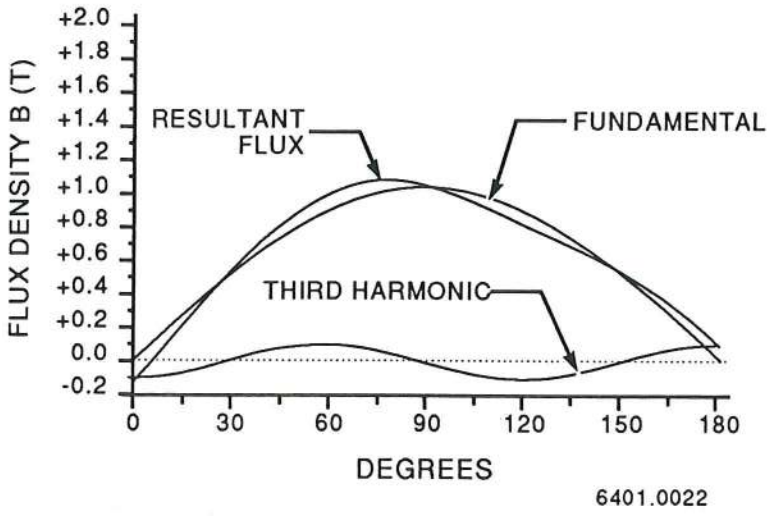
FLUX DENSITY B (T)
+2.0
+1.8
+1.6
+1.4
+1.2
+1.0
+0.8
+0.6
+0.4
+0.2
0.0
-0.2
RESULTANT FLUX
FUNDAMENTAL
THIRD HARMONIC
0
30
60
90
120
150
180
DEGREES
6401.0022

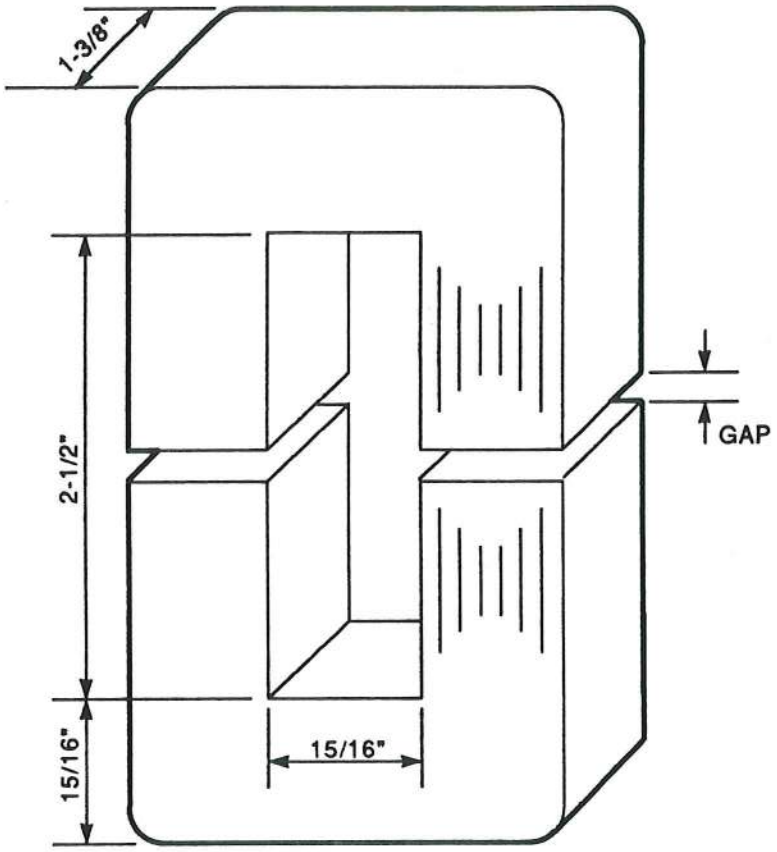

6401.0023

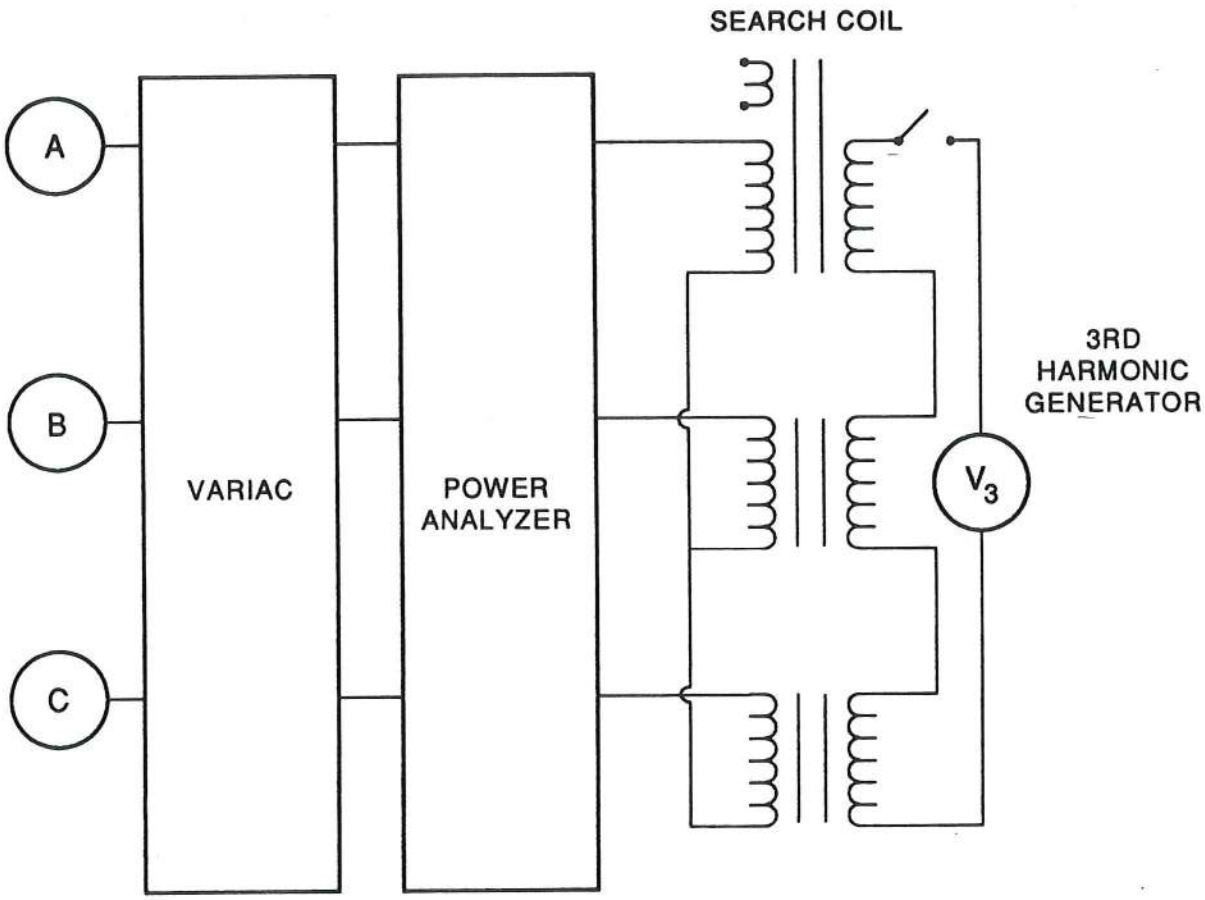
SEARCH COIL
A
B
C
VARIAC
POWER
ANALYZER
3RD
HARMONIC
GENERATOR
V_3

6401.0024

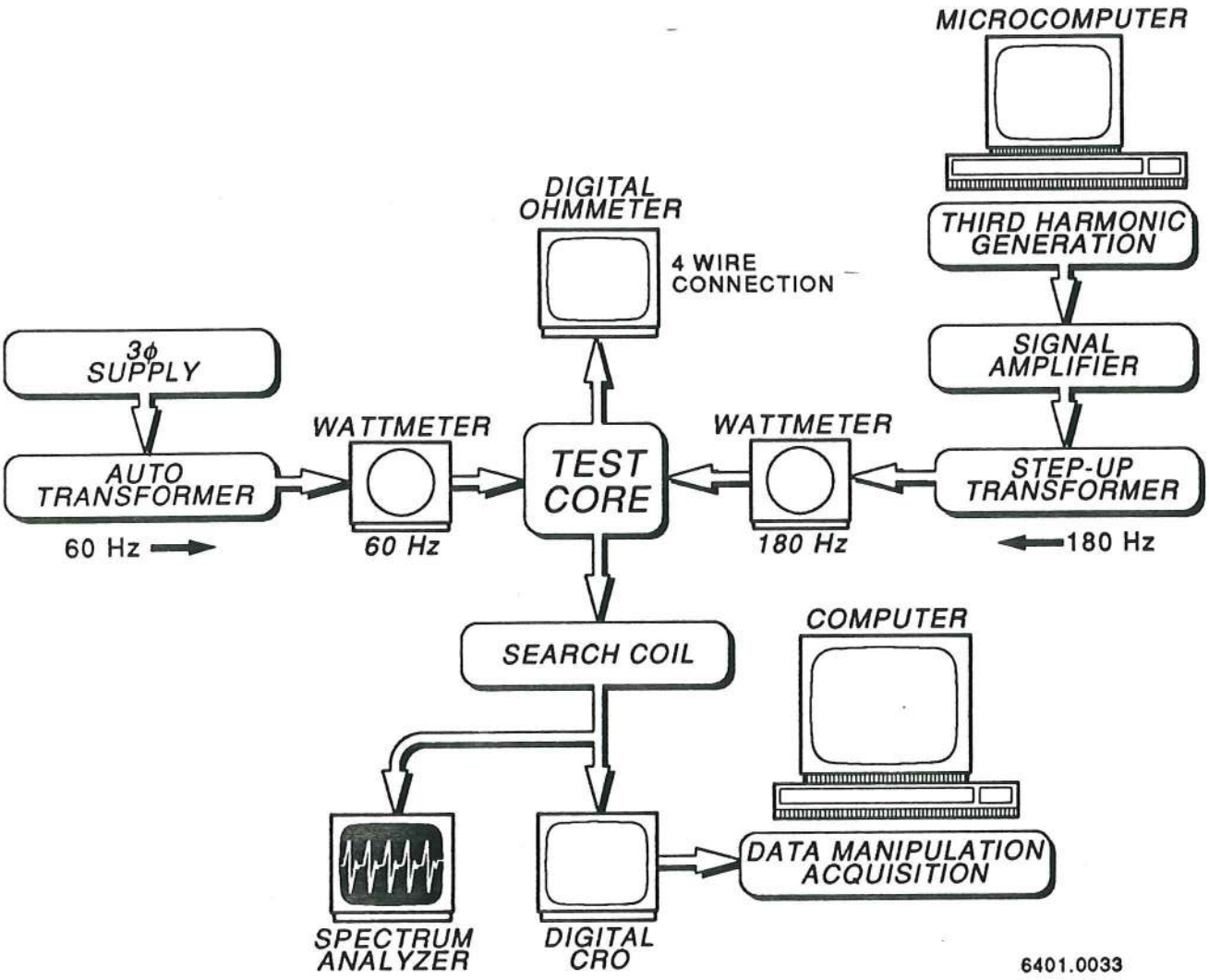
MICROCOMPUTER
DIGITAL OHMMETER
4 WIRE CONNECTION
THIRD HARMONIC GENERATION
SIGNAL AMPLIFIER
3φ SUPPLY
AUTO TRANSFORMER
60 Hz
WATTMETER
60 Hz
TEST CORE
WATTMETER
180 Hz
STEP-UP TRANSFORMER
180 Hz
SEARCH COIL
COMPUTER
DATA MANIPULATION ACQUISITION
SPECTRUM ANALYZER
DIGITAL CRO
6401.0033

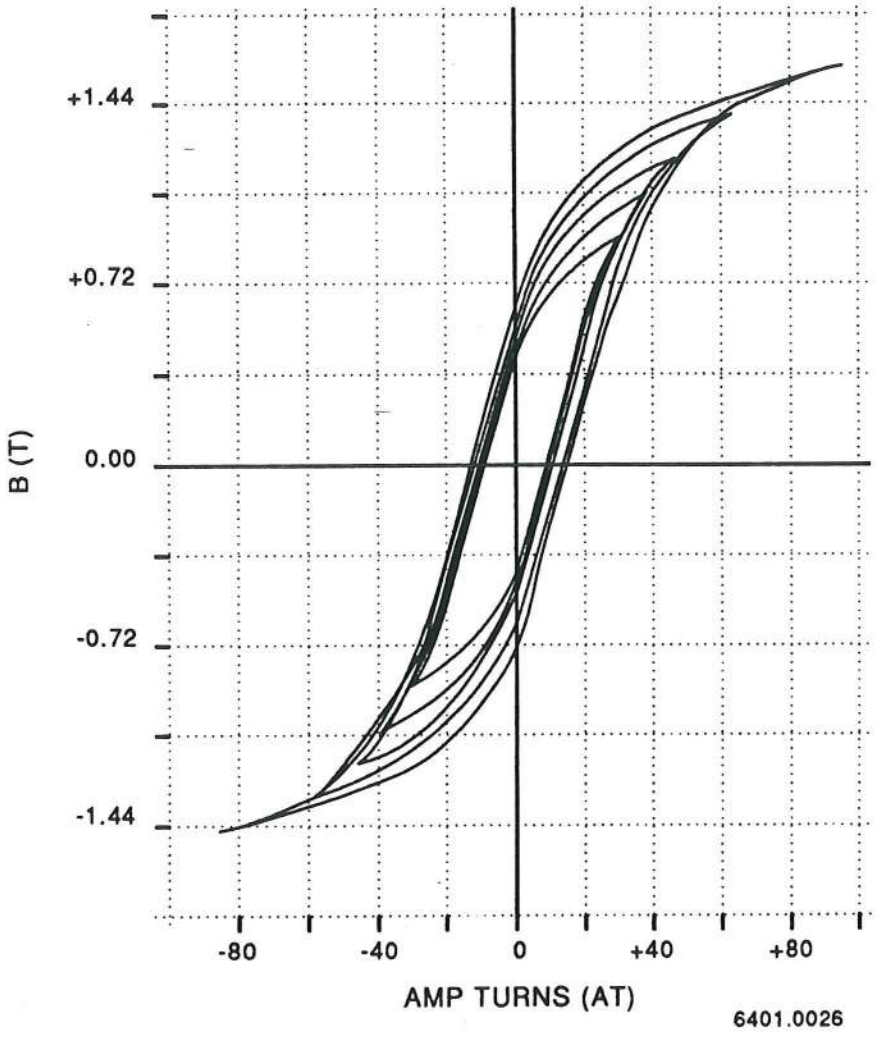
+1.44
+0.72
0.00
-0.72
-1.44
B (T)
-80
-40
0
+40
+80
AMP TURNS (AT)
6401.0026

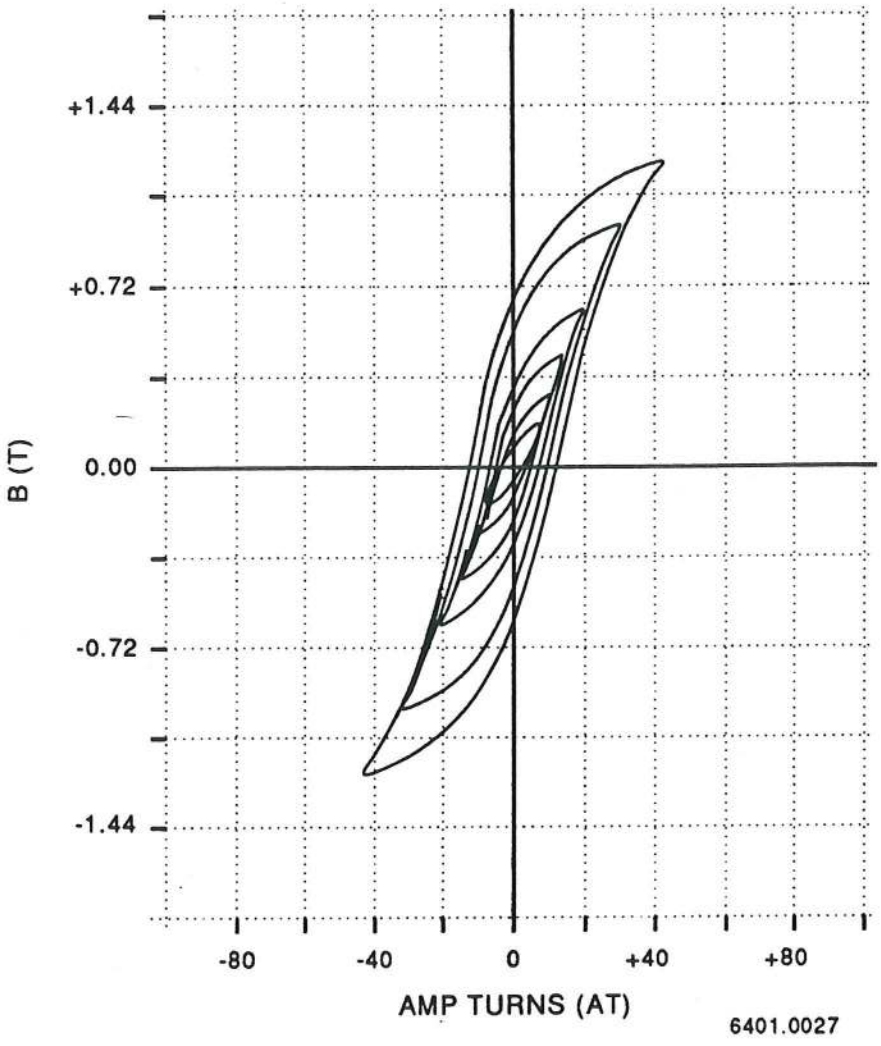
+1.44
+0.72
0.00
-0.72
-1.44
B (T)
-80
-40
0
+40
+80
AMP TURNS (AT)
6401.0027

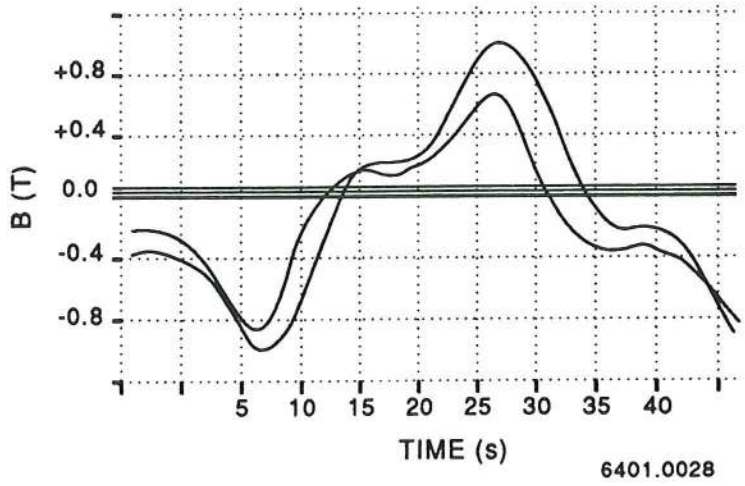
+0.8
+0.4
0.0
-0.4
-0.8
B (T)
5
10
15
20
25
30
35
40
TIME (s)
6401.0028

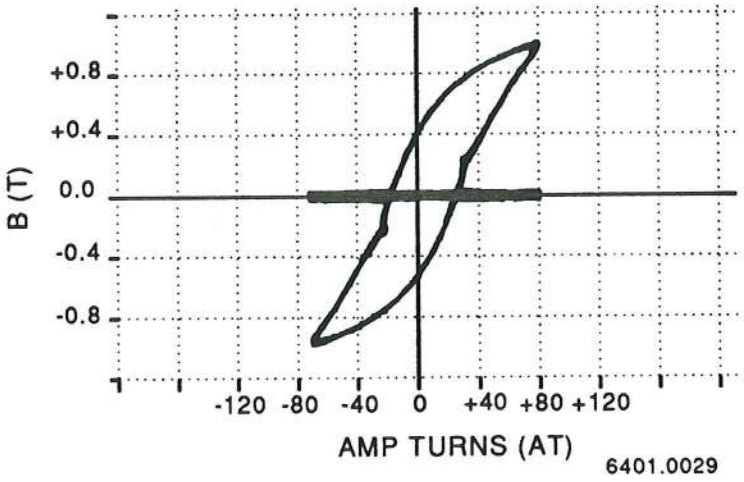
+0.8
+0.4
0.0
-0.4
-0.8
B (T)
-120 -80 -40 0 +40 +80 +120
AMP TURNS (AT)
6401.0029

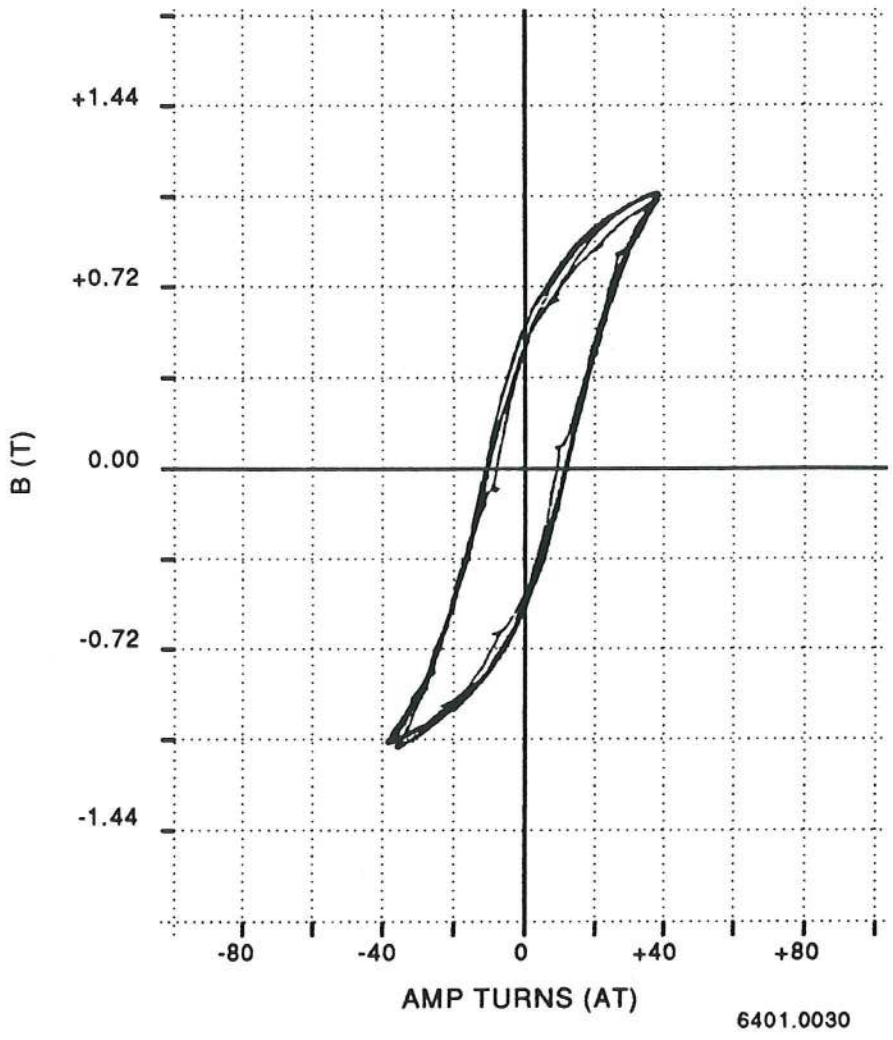
+1.44
+0.72
0.00
-0.72
-1.44
B (T)
-80
-40
0
+40
+80
AMP TURNS (AT)
6401.0030

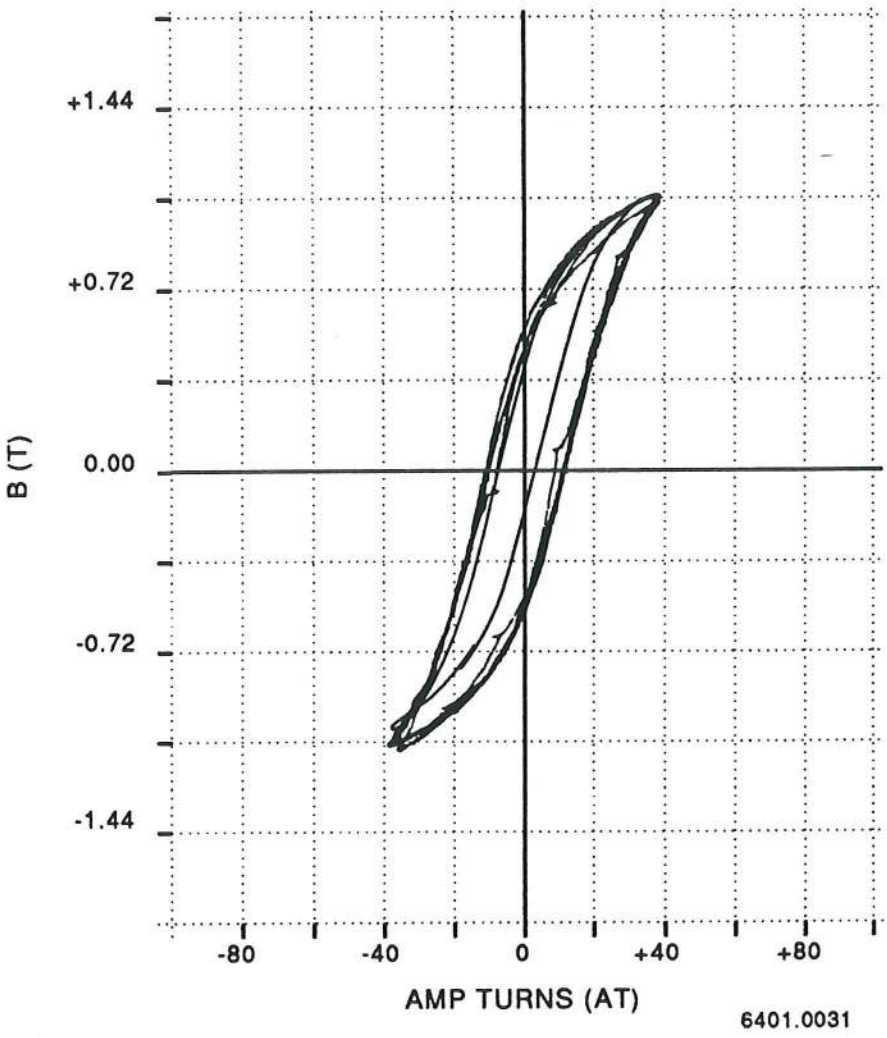
+1.44
+0.72
0.00
-0.72
-1.44
B (T)
-80
-40
0
+40
+80
AMP TURNS (AT)
6401.0031

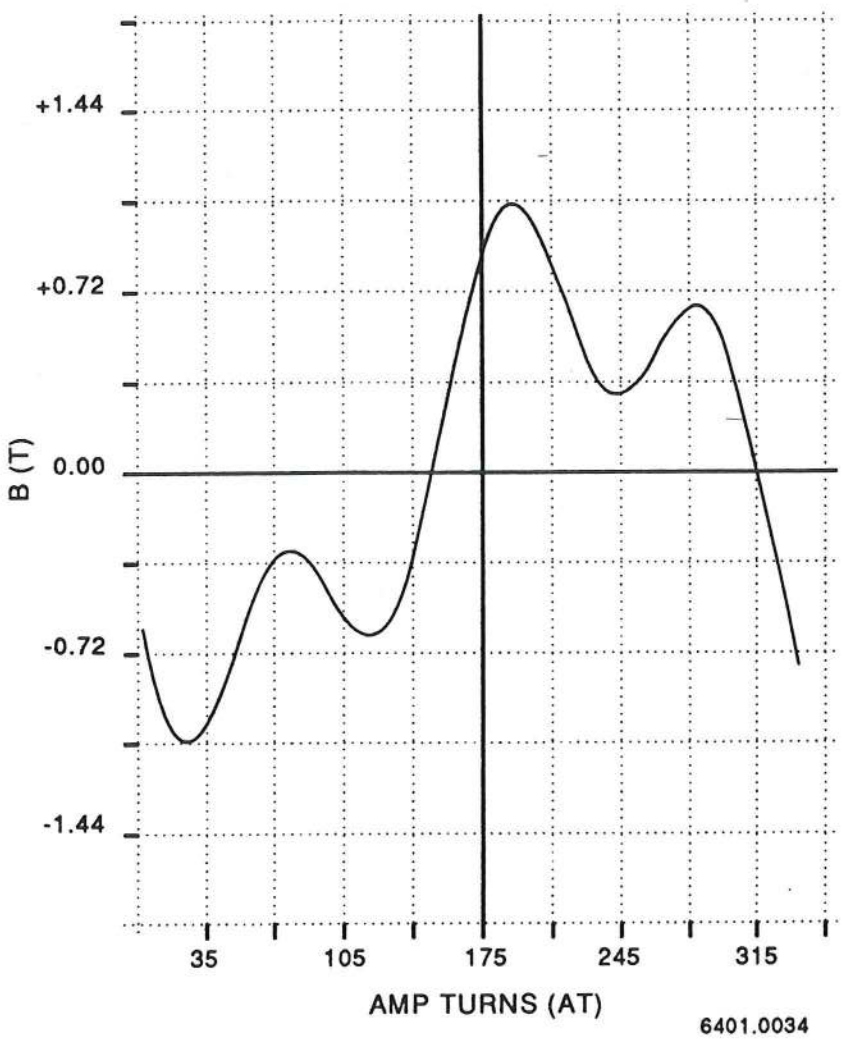
+1.44
+0.72
0.00
-0.72
-1.44
B (T)
35
105
175
245
315
AMP TURNS (AT)
6401.0034

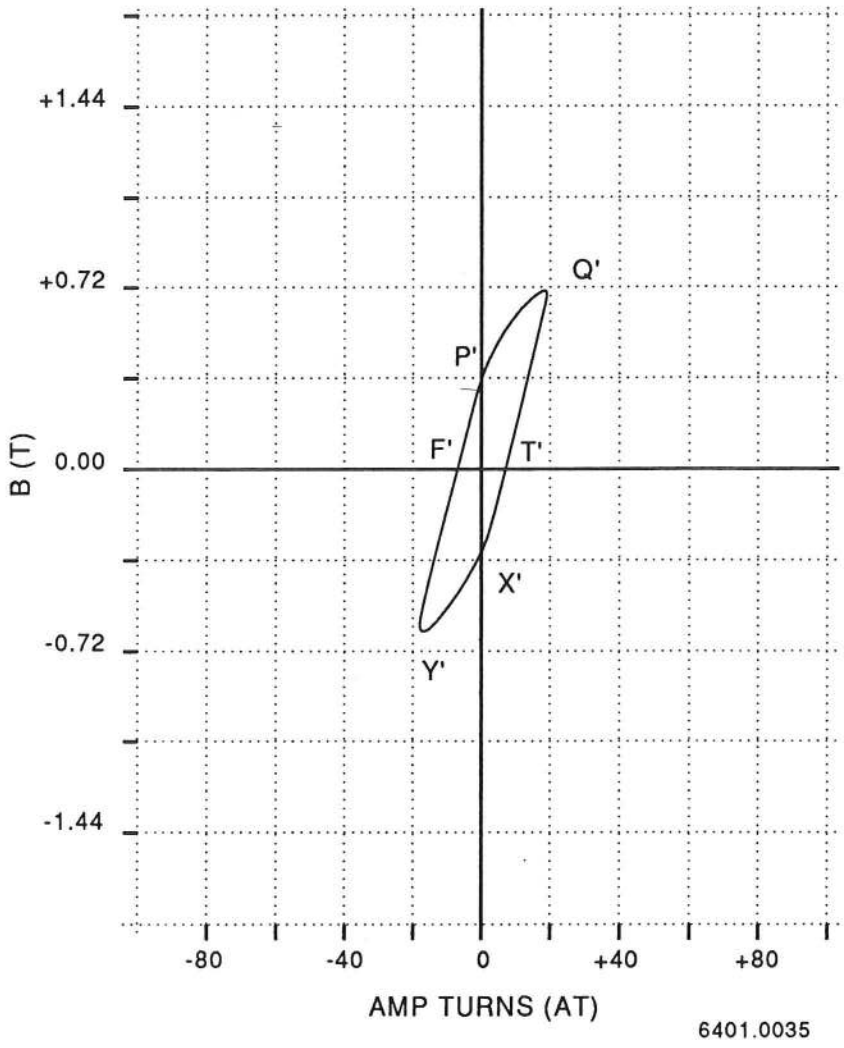
+1.44
+0.72
0.00
-0.72
-1.44
B (T)
Q'
P'
F'
T'
X'
Y'
-80
-40
0
+40
+80
AMP TURNS (AT)
6401.0035

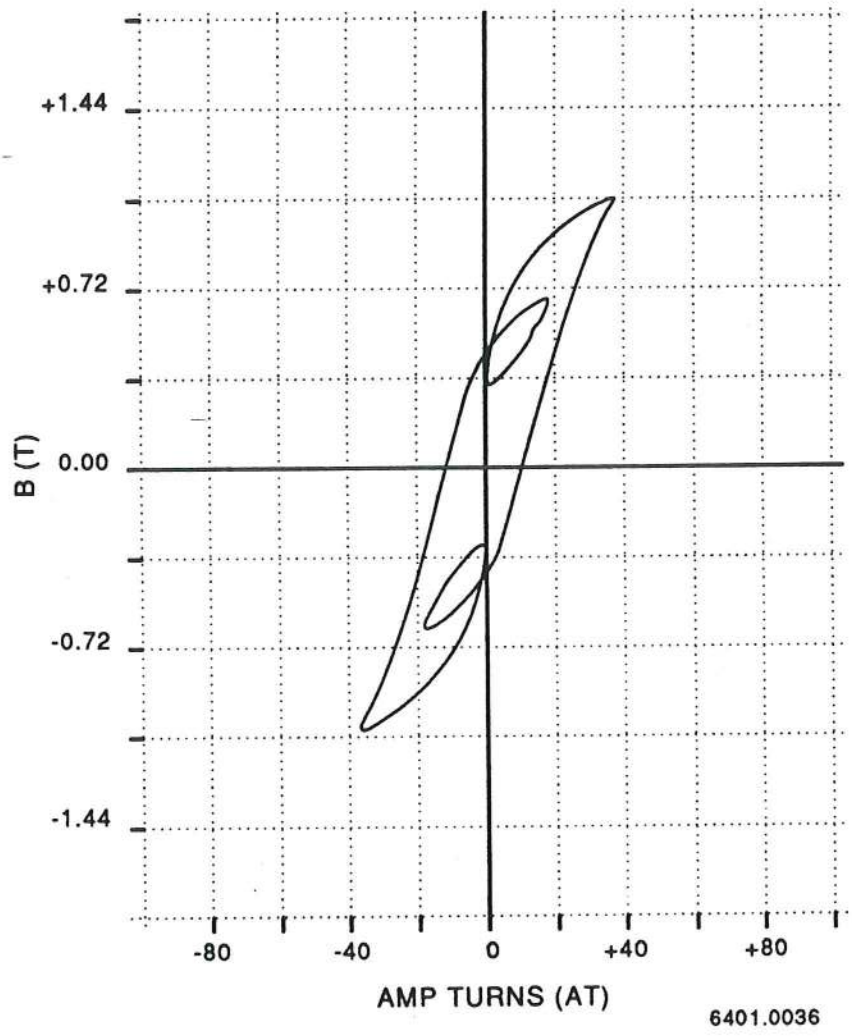
+1.44
+0.72
B (T)
0.00
-0.72
-1.44
-80
-40
0
+40
+80
AMP TURNS (AT)
6401.0036

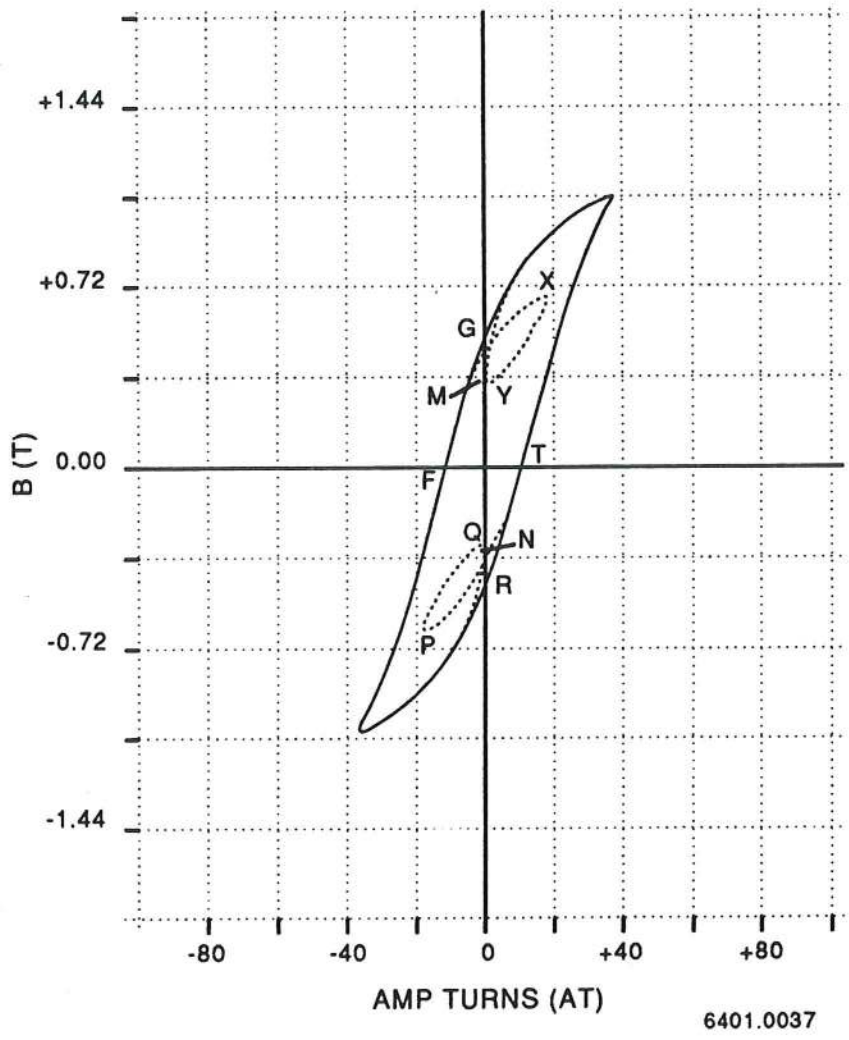
+1.44
+0.72
0.00
-0.72
-1.44
B (T)
-80
-40
0
+40
+80
AMP TURNS (AT)
X
G
M
Y
T
F
Q
N
R
P
6401.0037

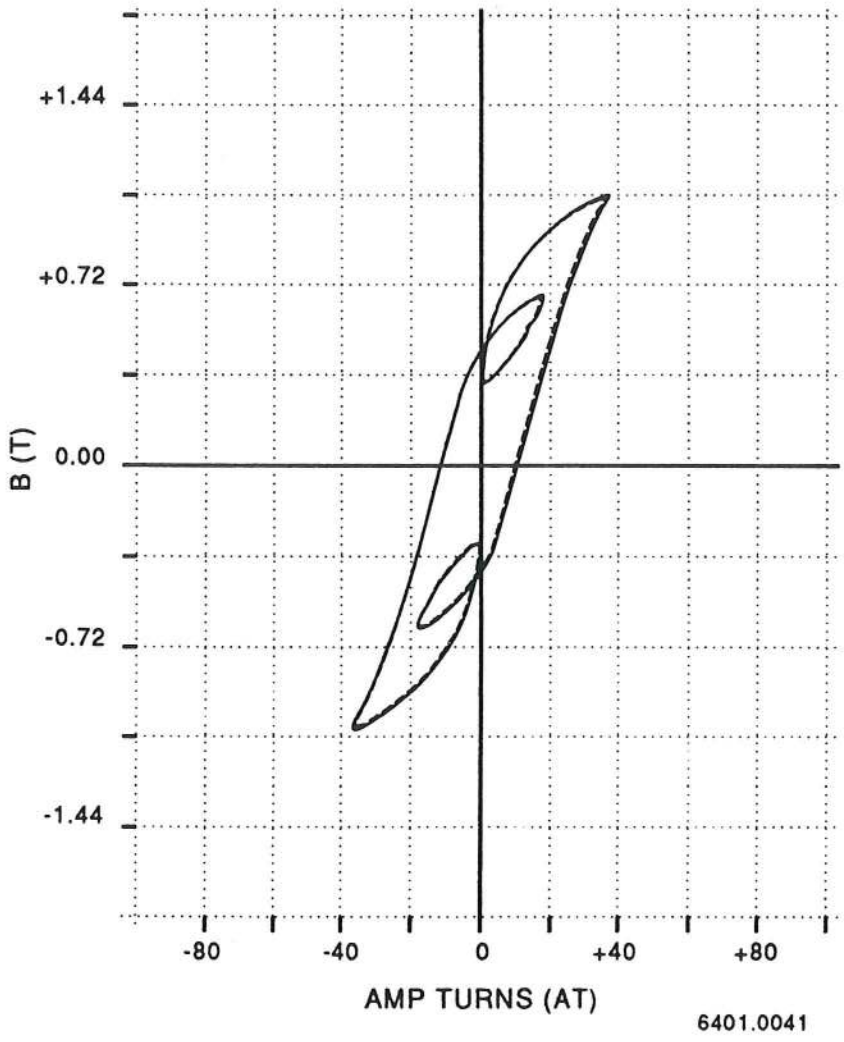
+1.44
+0.72
B (T)
0.00
-0.72
-1.44
-80
-40
0
+40
+80
AMP TURNS (AT)
6401.0041

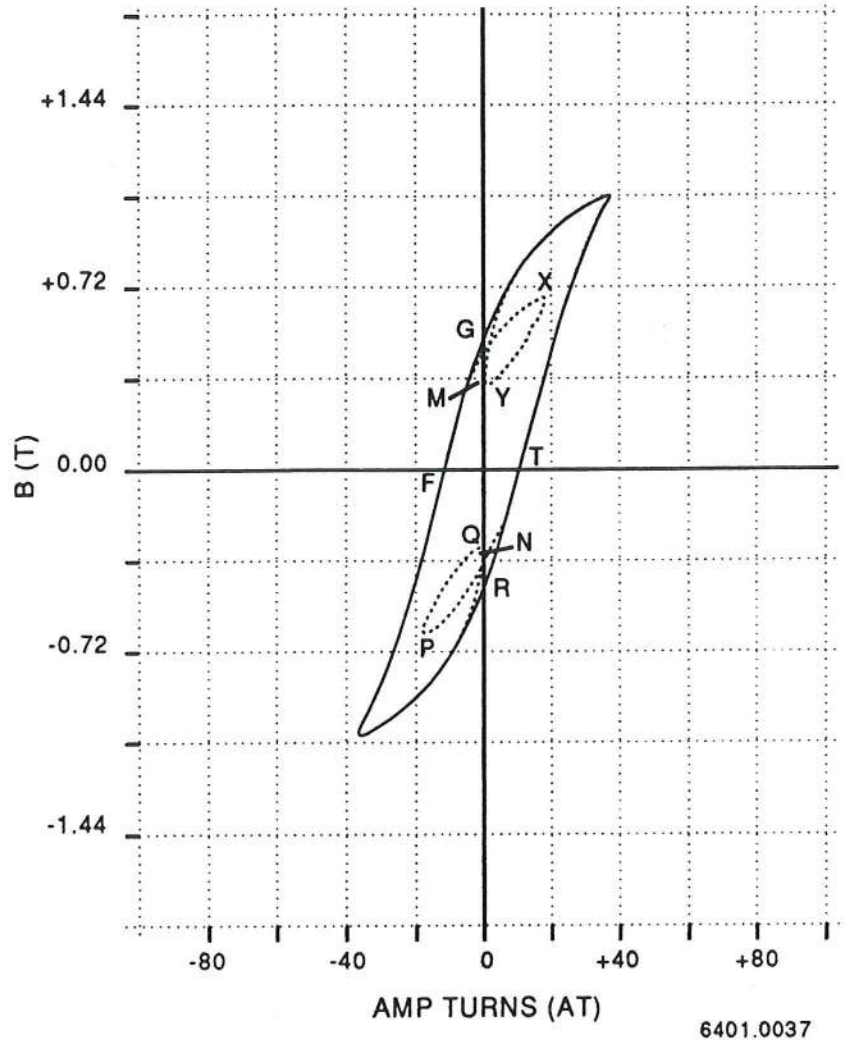
+1.44
+0.72
0.00
-0.72
-1.44
B (T)
-80
-40
0
+40
+80
AMP TURNS (AT)
X
G
M
Y
T
F
Q
N
R
P
6401.0037

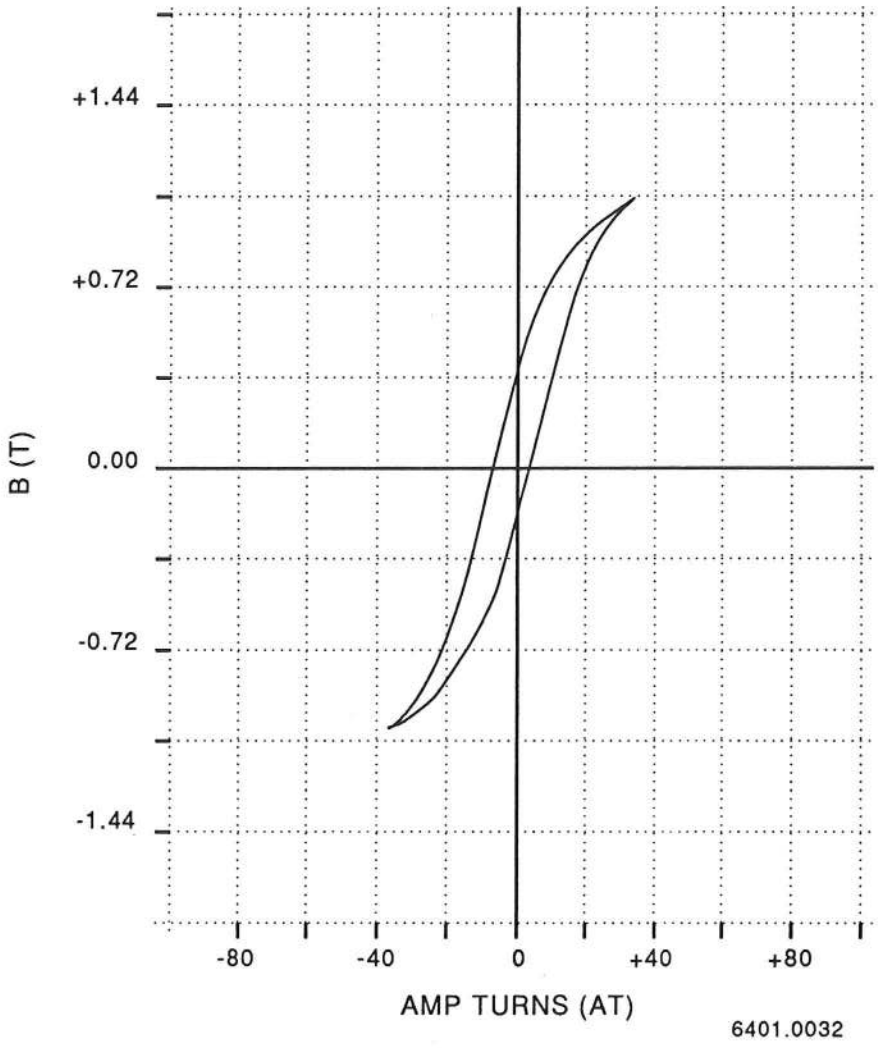
+1.44
+0.72
0.00
-0.72
-1.44
B (T)
-80
-40
0
+40
+80
AMP TURNS (AT)
6401.0032

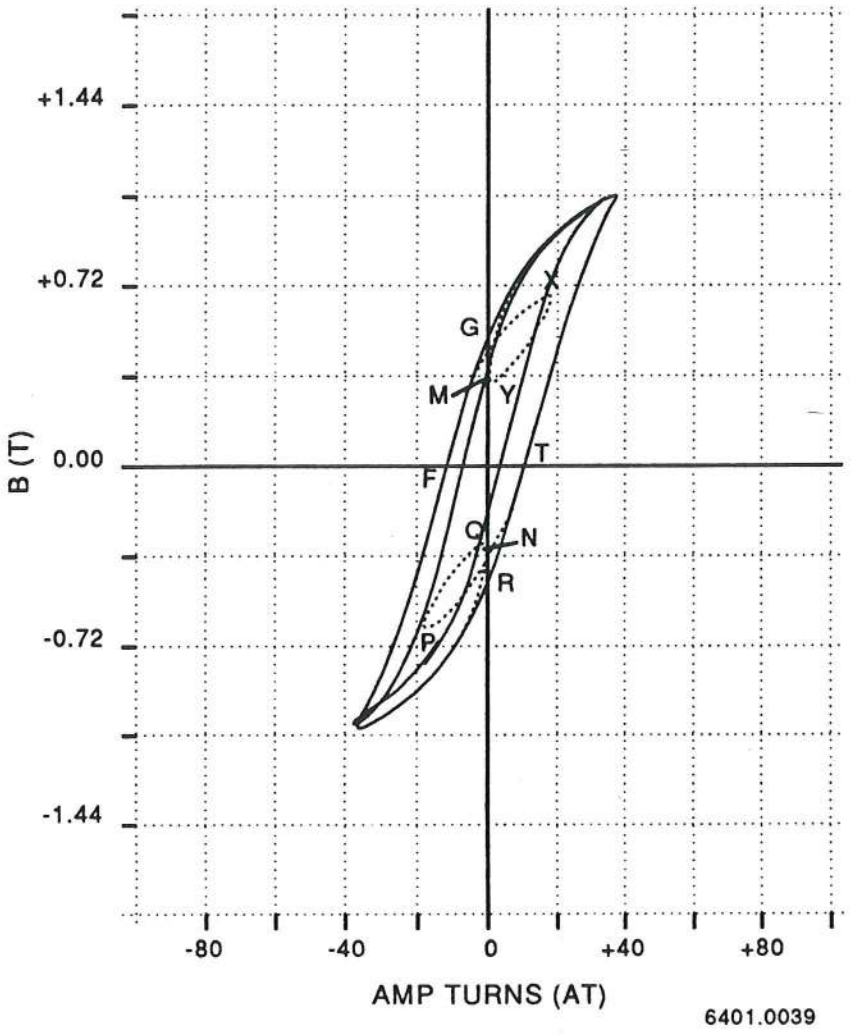
+1.44
+0.72
0.00
-0.72
-1.44
B (T)
-80
-40
0
+40
+80
AMP TURNS (AT)
G
M
Y
X
T
F
Q
N
R
P
6401.0039